



Ubiquitin- and ATP-dependent unfoldase activity of P97/VCP•NPLOC4•UFD1L is enhanced by a mutation that causes multisystem proteinopathy

Emily E. Blythe^a, Kristine C. Olson^{b,1}, Vincent Chau^b, and Raymond J. Deshaies^{a,c,2}

^aDivision of Biology and Biological Engineering, California Institute of Technology, Pasadena, CA 91125; ^bPennsylvania State University College of Medicine, Hershey, PA 17033; and ^cHoward Hughes Medical Institute, California Institute of Technology, Pasadena, CA 91125

Contributed by Raymond J. Deshaies, April 24, 2017 (sent for review April 14, 2017; reviewed by Peter K. Jackson and Robert T. Sauer)

p97 is a “segregase” that plays a key role in numerous ubiquitin (Ub)-dependent pathways such as ER-associated degradation. It has been hypothesized that p97 extracts proteins from membranes or macromolecular complexes to enable their proteasomal degradation; however, the complex nature of p97 substrates has made it difficult to directly observe the fundamental basis for this activity. To address this issue, we developed a soluble p97 substrate—Ub-GFP modified with K48-linked ubiquitin chains—for in vitro p97 activity assays. We demonstrate that WT p97 can unfold proteins and that this activity is dependent on the p97 adaptor NPLOC4-UFD1L, ATP hydrolysis, and substrate ubiquitination, with branched chains providing maximal stimulation. Furthermore, we show that a p97 mutant that causes inclusion body myopathy, Paget’s disease of bone, and frontotemporal dementia in humans unfolds substrate faster, suggesting that excess activity may underlie pathogenesis. This work overcomes a significant barrier in the study of p97 and will allow the future dissection of p97 mechanism at a level of detail previously unattainable.

AAA ATPase | Cdc48 | Npl4 | Ufd1 | Proteasome

The AAA ATPase p97, also called valosin-containing protein (VCP) or Cdc48 in yeast, is integral to a wide array of processes in the cell (1, 2). Its role in ER-associated degradation (ERAD) is the most well-studied, in which it functions to pull misfolded proteins from the ER membrane so they can be degraded by the proteasome (3). Other degradative pathways with substrates embedded in large structures, such as ribosome-associated degradation and mitochondrial-associated degradation, also rely on the activity of p97 (4–6). Furthermore, p97 is involved in nondegradative pathways like Golgi and nuclear envelope reassembly after mitosis and endosomal trafficking (7, 8). The common mechanism that underlies all these cellular jobs is presumed to be the extraction and unfolding of ubiquitylated proteins by p97 (9, 10). Its homology to other AAA ATPases that have demonstrated unfolding activities, such as the proteasome 19S regulatory particle (11, 12), ClpA (13), and VAT (14, 15), further support the model of p97 as an unfoldase. Although p97 has been shown to extract proteins from membranes and DNA, its ability to unfold a protein has not been explicitly demonstrated. Because of this considerable gap in our knowledge, the biochemical activity that underlies p97’s myriad functions remains a mystery.

Despite our poor molecular understanding of exactly what p97 does and how it does it, structural studies and indirect assays have provided some insight into p97 activity. p97 is a homohexamer, with each protomer comprising an N-domain, two ATPase domains (D1 and D2) stacked one upon the other, and an unstructured C-terminal tail (16–18). Although both ATPase domains are functional, it is thought that hydrolysis of ATP in D2 is the main driver of mechanical force and ATP binding in D1 promotes hexamer formation (19–25). The conformations of the two ATPase domains and the N-domain with respect to one another are highly cooperative and dependent upon nucleotide binding and hydrolysis (17, 18, 20, 22, 26–32). Recent high-resolution structural studies show movement of D2 relative to N-D1 upon ATP binding in D2, whereas the N domains move

from a coplanar to an axial position with respect to D1 upon ATP binding to D1 (18). It is unclear how these conformational changes translate to mechanical force for remodeling protein substrates. Homologs like ClpA function by threading polypeptides through the central pore (33), and, even though p97 lacks the requisite hydrophobic pore residues in D1, other pore residues interact with and are key to the processing of substrates (19, 34). However, structural studies imply that the central pore of p97 may be too narrow to accommodate a polypeptide (16, 18). Other proposed mechanisms include unfolding by D2 through the arginine “denaturation collar” and unfolding outside of the pore by the movement of the N-domains, similar to what has been proposed for NSF (34, 35). Resolution of the key question of how p97 works has been stymied by the lack of a direct assay to measure the core biochemical activity underlying its “segregase” function.

In performing its biological functions, p97 does not act alone but instead associates with a set of adaptor proteins that act to recruit or modify substrates (36). Many of the adaptors contain ubiquitin (Ub)-binding domains or can add or remove ubiquitin modifications, thereby linking p97 to ubiquitin signaling (36, 37). Some adaptors also modulate p97 ATPase activity (38–40). Whereas a few adaptors have been linked to specific pathways or substrates (8, 41–44), the functions of others remain unknown (36, 37). The best-characterized p97 adaptor is the heterodimer of NPLOC4/Npl4 and UFD1L/Ufd1 (UN), which recruits substrates in ERAD and other

Significance

The ATPase p97 plays an important cellular role by extracting proteins modified with ubiquitin (Ub) from membranes, chromatin, or protein complexes. However, the unstable and complicated nature of p97 substrates has hindered a detailed study of mechanism. To overcome these issues, we developed Ub-GFP as a fluorescent reporter of p97 activity. When Ub-GFP is conjugated with ubiquitin chains, p97 and its cofactor NPLOC4-UFD1L unfold it in an ATP-dependent manner, explicitly demonstrating that p97 is an unfoldase. We also show that a p97 mutation associated with multisystem proteinopathy has enhanced unfoldase activity, which suggests a novel approach to disease therapy. Our method opens the door for future studies of p97 mechanism that were until now not feasible.

Author contributions: E.E.B. and R.J.D. designed research; E.E.B. performed research; K.C.O. and V.C. contributed new reagents/analytic tools; E.E.B. and R.J.D. analyzed data; and E.E.B. and R.J.D. wrote the paper.

Reviewers: P.K.J., Stanford University; and R.T.S., Massachusetts Institute of Technology.

Conflict of interest statement: R.J.D. is a founder and a shareholder of Cleave Biosciences, which is developing CB-5083 for therapy of cancer. The other authors declare that no competing interests exist.

¹Present address: Division of Hematology and Oncology, Department of Medicine, University of Virginia, Charlottesville, VA 22908.

²To whom correspondence should be addressed. Email: deshaies@caltech.edu.

This article contains supporting information online at www.pnas.org/lookup/suppl/doi:10.1073/pnas.1706205114/-DCSupplemental.

proteasome-dependent degradative processes (45–47). NPLOC4 and UFD1L each bind ubiquitin chains, with UFD1L showing specificity for K48-linked chains (25, 48, 49). They interact with p97 at separate sites to form a complex with the stoichiometry of one UN heterodimer per p97 hexamer (39, 46, 50–52).

A significant incentive to gaining a deeper understanding of p97's mechanism of action is the deep connection between this protein and human disease and possibly cancer therapy. Human p97 is mutated in the inherited, autosomal-dominant multisystem proteinopathy known as inclusion body myopathy associated with Paget disease of bone and/or frontotemporal dementia (IBMPFD) (53, 54). In addition, a small fraction of patients with inherited amyotrophic lateral sclerosis (ALS; also known as Lou Gehrig's disease) also carry mutations in p97 that overlap with those seen in patients with IBMPFD (54, 55). However, the mechanism of pathogenesis is not understood in either case. It has been suggested at various times that pathogenesis arises from a failure of autophagy, endosomal sorting, clearance of leaky lysosomes, mitochondrial homeostasis, or mTOR regulation (8, 56–61). Regardless of the cellular target, the molecular-level defect remains obscure. It has been suggested that failure of mutant p97 to bind UBXLN6/UBXD1 is key (8), but IBMPFD mutants also show increased binding of UN (62). The mutations that cause IBMPFD all fall within the N-D1 domain interface and affect the relative orientation of these domains (63–66). Moreover, the mutations cause elevated ATP hydrolysis (20, 63–65, 67), but it has been suggested that this is an indirect consequence of a decoupling of substrate binding from mechanochemical transduction in the D2 domain (54, 68). Because p97 is a hexamer, it has been unclear how to interpret the autosomal-dominant nature of IBMPFD. Is this truly the result of enhanced activity, or do the mutations actually cause reduction of function through a dominant-negative mechanism, with mutant protomers poisoning mixed hexamers? Studies in *Drosophila* support the idea that the pathogenesis of IBMPFD mutations stems from elevated p97 activity, resulting in increased processing of TDP-43 (69) and mitofusin (61). As of yet, there remains no biochemical assay that measures p97's presumed core function of protein unfolding that would enable a direct test of this hypothesis in a defined system.

The nature of the majority of known p97 substrates—unstable, scarce, modified by ubiquitin, and not readily divorced from their contexts—presents challenges for studying the enzymatic activity of p97 in a systematic manner. A major barrier to progress has been the absence of a simple, rapid, quantitative assay that uses defined components and can be used to dissect in detail the mechanism of action of p97. To address this obstacle, we have developed a soluble, monomeric p97 substrate. Our substrate is based on a noncleavable ubiquitin fusion protein, Ub^{G76V}GFP, which is targeted for proteolysis by the ubiquitin fusion degradation (UFD) pathway (70). Normally, ubiquitin fusions are cotranslationally cleaved by a deubiquitinating enzyme to remove the ubiquitin (71). However, if the C-terminal glycine is mutated, processing is blocked and the fusion is rapidly degraded. Previous studies have demonstrated that the degradation of these noncleavable ubiquitin fusion proteins, including Ub^{G76V}GFP, is dependent upon p97•UN in human, *Drosophila*, and yeast cells (19, 47, 70, 72). We show that p97 can unfold Ub^{G76V}GFP modified with a K48-linked polyubiquitin chain and that this reaction is dependent upon the nature of the ubiquitin chain, UN, and p97 ATPase activity in D2. Our system provides a direct demonstration of a p97 unfoldase activity that depends on predicted physiological requirements and will be an invaluable tool for further study of p97's mechanism.

Results

Substrate and Assay Design. We chose to pursue the UFD pathway substrate Ub^{G76V}GFP because it is rapidly degraded in a p97-dependent manner in yeast, *Drosophila*, and human cells (19)

and is a well-behaved protein whose folding state can be easily monitored by fluorescence. As p97 substrates are often polyubiquitylated, and p97•UN binds polyubiquitin (25), we reasoned that Ub^{G76V}GFP would need to be polyubiquitylated to be recognized. To efficiently ubiquitylate it, we developed a chimera of the RING domain from the E3 ubiquitin ligase gp78 and the E2 enzyme Ube2g2. Prior studies have shown that these enzymes catalyze formation of K48-linked ubiquitin chains (25). Notably, these two enzymes function upstream of p97 in ERAD, attesting to the physiological relevance of the use of these enzymes to generate a p97 substrate for our assay (73, 74). Compared with Ube2g2 alone or unfused Ube2g2 with added gp78RING (Fig. S1A), the gp78RING-Ube2g2 chimera produced unanchored polyubiquitin chains with very high efficiency (Fig. S1B).

Using this tool, we used various strategies to produce three types of potential p97 substrates. To simplify notation, linearly fused proteins are shown by dashes, and the length of the K48-linked ubiquitin chain attached to a particular ubiquitin is shown with a superscript preceding the initiator ubiquitin. First, we aimed to create a substrate with a short ubiquitin chain of defined length. Although the minimal requirement for recognition of ubiquitylated proteins by p97 is not known, the minimum ubiquitin chain length for recognition by the proteasome is four (75). Therefore, we enzymatically ligated Ub₃, in which the ubiquitins were joined via K48 linkages and the distal ubiquitin carried a K48R mutation, onto the linearly fused ubiquitin to form pure Ub³Ub-GFP (Fig. 1A) (76, 77). Second, to create a substrate with longer polyubiquitin chains, we built K48-linked chains directly onto the linearly fused ubiquitin (Fig. 1B). Finally, to produce substrate with branched ubiquitin chains, we built ubiquitin chains on a base substrate containing two or more linearly fused ubiquitins (Ub-Ub-GFP or Ub-Ub-Ub-GFP; Fig. 1C). Heterogeneous substrates were fractionated by size-exclusion chromatography to enrich for different chain lengths (Fig. 1D).

One concern we had was the potential for GFP to refold after being processed by p97, leaving the assay without an observable endpoint. To address this, we added an ATPase mutant of the chaperonin GroEL. The GroEL D87K “trap” retains the ability to bind unfolded proteins but can no longer release those proteins (78). This dead-end complex sequesters unfolded GFP, preventing it from refolding, and has been used previously to provide assay endpoints for other unfolding machines (13).

GFP Is Unfolded by p97 in a Ubiquitin- and UN-Dependent Manner. To explore the unfolding potential of p97, we first compared a set of Ub-GFP substrates bearing K48-linked ubiquitin chains of varying lengths (Fig. 2A). When mixed with p97, UN, and GroEL (Fig. S2), Ub-GFP and Ub³Ub-GFP showed no appreciable loss of GFP fluorescence (Fig. 2B). However, Ub-GFP with both “medium” (>4 ubiquitins; Ub^MUb-GFP) and “long” (>12 ubiquitins; Ub^LUb-GFP) ubiquitin chains showed a modest decrease in fluorescence over time (~30%; Fig. 2B). Whereas Ub^LUb-GFP did show improved unfolding relative to Ub^MUb-GFP, the difference was quite small (~5% signal loss).

We examined further the requirements for p97-dependent unfolding by using Ub^LUb-GFP, as this substrate gave the largest signal. When incubated with only p97 or p97 and GroEL, no unfolding was observed (Fig. 2C). A similar result was obtained when UN was replaced with NSFL1C/p47 or UBXLN7/UBXD7, p97 adaptors involved in Golgi reassembly after mitosis (41) and regulation of cullin-RING ubiquitin ligases (37, 43, 79), respectively, despite both of these adaptors binding to p97 and substrate (Fig. S3). Therefore, UN is required for p97-catalyzed unfolding, and it cannot be replaced by other adaptors. Additionally, GroEL was essential to provide an endpoint for the assay. Fluorescence loss was amplified by the addition of GroEL (Fig. 2C), indicating that GFP was able to refold to some degree after processing by p97•UN. However, GroEL did not unfold substrate on its own

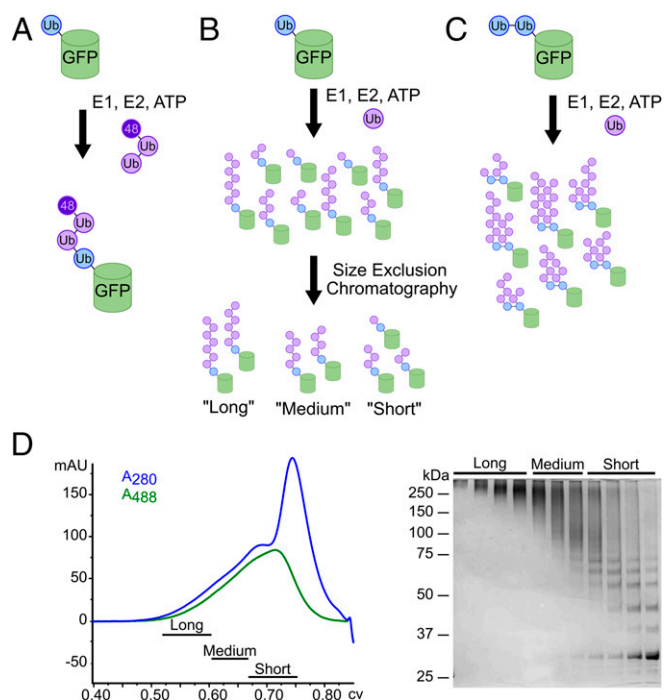


Fig. 1. Substrate design and synthesis. (A) Preassembled, K48-linked Ub₃ chains containing a K48R mutation on the distal ubiquitin were ligated onto a noncleavable linear His₆-Ub-GFP fusion protein to produce pure Ub₃Ub-GFP. (B) E1, E2, ubiquitin, and ATP were added to His₆-Ub-GFP to elongate K48-linked ubiquitin chains of varying lengths on the ubiquitin fused to GFP. These resulting substrates were purified from free ubiquitin chains via Ni-NTA resin and crudely fractionated according to chain length via size-exclusion chromatography to produce pools of “long-”, “medium-”, and “short-”-chain substrates (Ub^LUb-GFP, Ub^MUb-GFP, and Ub^SUb-GFP, respectively). (C) To produce branched chains, ubiquitin chains of varying length were enzymatically elongated on a di- or triubiquitin linear fusion protein, Ub-Ub-GFP, or Ub-Ub-Ub-GFP, similar to B. (D) Size-exclusion chromatogram and corresponding SDS/PAGE gel for the purification of substrate described in B.

(Fig. 2C), and immunoprecipitation (IP) of GroEL showed that p97•UN was required for GroEL interaction with substrate (Fig. 2D). Unfolding of substrate by p97 was also highly temperature-dependent, with the rate and extent of unfolding increasing between 22 °C and 42 °C (Fig. S4).

We found it curious that $\leq 40\%$ of the fluorescence signal of Ub^LUb-GFP was typically lost in our unfolding assays even though all components of the system were at or very near saturation (Fig. S5), suggesting that there was another factor influencing substrate competence that remained to be discovered. Three ubiquitin binding sites with different chain linkage preferences are available on p97•UN (25). Therefore, we tested whether substrates carrying branched ubiquitin chains would be more effectively unfolded, because a branch would enable two separate ubiquitin chains to be elaborated from a single attachment point (in this case, Met1 of GFP). As a proxy for ubiquitin chains with branched linkages, we expressed Ub-GFP fused to one or more additional ubiquitins in tandem and used these proteins as substrates for subsequent enzymatic polyubiquitylation (Fig. 3A). Interestingly, a substrate in which K48-linked polyubiquitin chains were polymerized on Ub-Ub-GFP (Ub^MUb-Ub-GFP) showed significant improvement in unfolding by p97 compared with Ub^MUb-GFP (Fig. 3B) despite the latter having a greater amount of ubiquitin conjugation as judged by mobility upon SDS/PAGE (Fig. 3A, lanes 1 and 2). Neither further extension of the chains to form Ub^LUb-Ub-GFP nor use of a triubiquitin fusion significantly increased the rate or extent of unfolding (Fig. 3B).

Although we cannot directly visualize ubiquitin chains branching from each ubiquitin in the Ub-Ub-GFP fusion protein, reactions run with Ub-K48R indicate that both ubiquitin moieties were efficiently conjugated with ubiquitin under our reaction conditions (Fig. S6). Incidentally, this same reaction confirms the linkage specificity of our Ube2g2-gp78 E2-E3 chimera. Taken together, our data suggest that the physical arrangement of the ubiquitin chains is important for unfolding by p97•UN, with the enzyme preferring substrates with at least one branch point that enables nucleation of more than one chain of K48-linked ubiquitins.

Substrate Unfolding Is Dependent upon ATP Hydrolysis and Stimulates p97 ATPase Activity. Next, we examined the energy-dependence of p97-catalyzed unfolding. Ub^LUb-Ub-GFP was not unfolded by p97 in the absence of nucleotide, and ADP or the nonhydrolyzable ATP analog ATPγS could not substitute for ATP (Fig. 4A). Two p97 ATPase inhibitors, the allosteric inhibitor NMS-873 (80) and the D2-specific, ATP-competitive inhibitor CB-5083 (81), also prevented ATP-dependent substrate processing (Fig. 4A). p97 with a D1 domain Walker B motif mutation (p97-E305Q) that blocks nucleotide hydrolysis but not binding exhibited only mild defects in substrate unfolding. By contrast, the same mutation in D2 (p97-E578Q) completely abolished unfoldase activity (Fig. 4B and Table 1). Together, these data demonstrate that ATP hydrolysis in D2 powers the unfolding of substrate by p97•UN.

Some adaptors modulate p97 ATPase activity (38), so we examined the effects of substrate processing on the hydrolysis of ATP by p97 and p97•UN. Addition of long unanchored K48-linked ubiquitin chains (Ub^LUb), Ub-GFP, Ub^SUb-GFP, or Ub^LUb-Ub-GFP did not alter the ATPase activity of p97 (Fig. S7A).

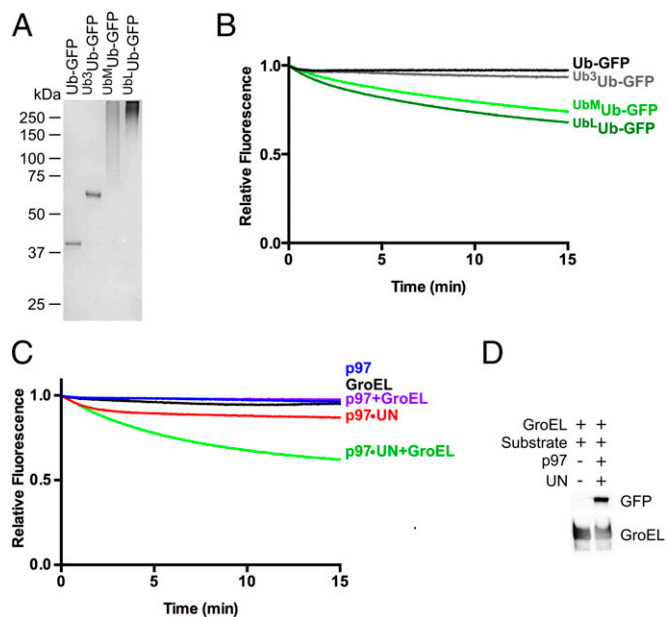


Fig. 2. p97 unfolds Ub-GFP in a UN-dependent manner (A) SDS/PAGE analysis of GFP substrates with different ubiquitin chain structures stained with Coomassie Brilliant Blue. (B) Upon addition of ATP, 75 nM p97, 150 nM UN, and 250 nM GroEL, 25 nM Ub-GFP, and Ub^SUb-GFP did not appreciably lose fluorescence over time. However, Ub-GFP with “medium” or “long” K48-linked chains (Ub^MUb-GFP and Ub^LUb-GFP) exhibited 26% and 32% loss of signal after 15 min, respectively. Representative traces shown ($n \geq 3$). (C) Fluorescence of Ub^LUb-GFP did not change over time with the addition of p97, GroEL, or p97 plus GroEL. Upon addition of p97 plus UN, a small decrease in signal was observed, and this decrease was augmented with the addition of GroEL. Representative traces shown ($n \geq 2$). (D) Ub^LUb-GFP coimmunoprecipitated with GroEL only in the presence of p97 and UN.

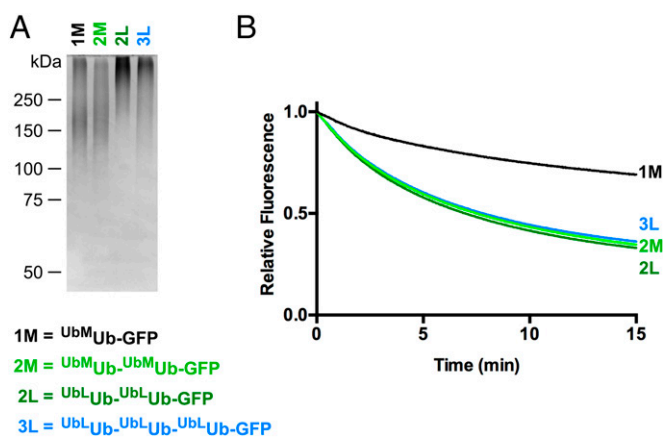


Fig. 3. Branched ubiquitin chains are better p97 substrates. (A) SDS/PAGE analysis of Ub-GFP substrates stained with Coomassie Brilliant Blue. (B) Comparison of unfolding of substrates with one, two, or three ubiquitins fused in tandem to GFP. Note that substrate with two linearly fused ubiquitins (e.g., $U^{bM}Ub-U^{bM}Ub-GFP$) was unfolded to a greater extent by p97 than substrate with a single linearly fused ubiquitin even though aggregate ubiquitination for the latter substrate was at least as extensive or greater than the former. Addition of an additional linearly fused ubiquitin ($U^{bL}Ub-U^{bL}Ub-U^{bL}Ub-GFP$) yielded no further improvement. Representative traces shown ($n \geq 3$).

Whereas UN did not significantly affect the ATPase activity of p97, the further addition of $U^{bL}Ub-U^{bL}Ub-GFP$ stimulated ATP hydrolysis by approximately fourfold, whereas Ub-GFP and $U^{b3}Ub-GFP$ had no effect (Fig. 4C). The latter result is consistent with the

inability of p97•UN to unfold Ub-GFP or $U^{b3}Ub-GFP$. Neither NSFL1C nor UBXM7 supported substrate-triggered acceleration of p97 ATP hydrolysis (Fig. S7B). Long, unanchored ubiquitin chains also stimulated p97 ATPase activity to a similar degree as $U^{bL}Ub-U^{bL}Ub-GFP$, suggesting that p97 interaction with ubiquitin chains and not the GFP substrate itself was necessary and sufficient for the observed acceleration. In agreement with the unfolding results, the residual ATPase activity of p97-E578Q was unaffected by substrate plus UN (Fig. 4D). However, p97-E305Q, which was able to unfold substrate, was also not stimulated by substrate, and even showed a slight decrease in ATPase activity (Fig. 4D). The E305Q mutant also showed higher basal ATPase activity than WT, as has been seen before in steady-state experiments (20). These results suggest that there is a high degree of cross-talk between ATPase activity in D1 and D2, and whereas ATP hydrolysis in D2 is the driving force for unfolding, D1 activity is also needed for substrate-induced ATPase acceleration.

UN Recruits Substrate to p97. The tight correlation between the competence of a substrate to be unfolded and its ability to accelerate ATP hydrolysis suggests that binding of substrate to p97 may stimulate ATPase activity, leading to substrate unfolding. To further probe this hypothesis, we evaluated binding of substrate to p97. IP of p97 showed that it bound $U^{bL}Ub-U^{bL}Ub-GFP$ substrate in the presence but not in the absence of UN (Fig. 5A, lanes 4 and 5). Reciprocal IP of GFP confirmed that substrate bound UN in the absence of p97 but did not bind p97 in the absence of UN (Fig. 5B). Furthermore, the interaction between p97 and UN appeared to be stabilized by substrate binding (Fig. 5A, lanes 3 and 5). We also analyzed substrate dependence of GroEL association with p97, but observed high background

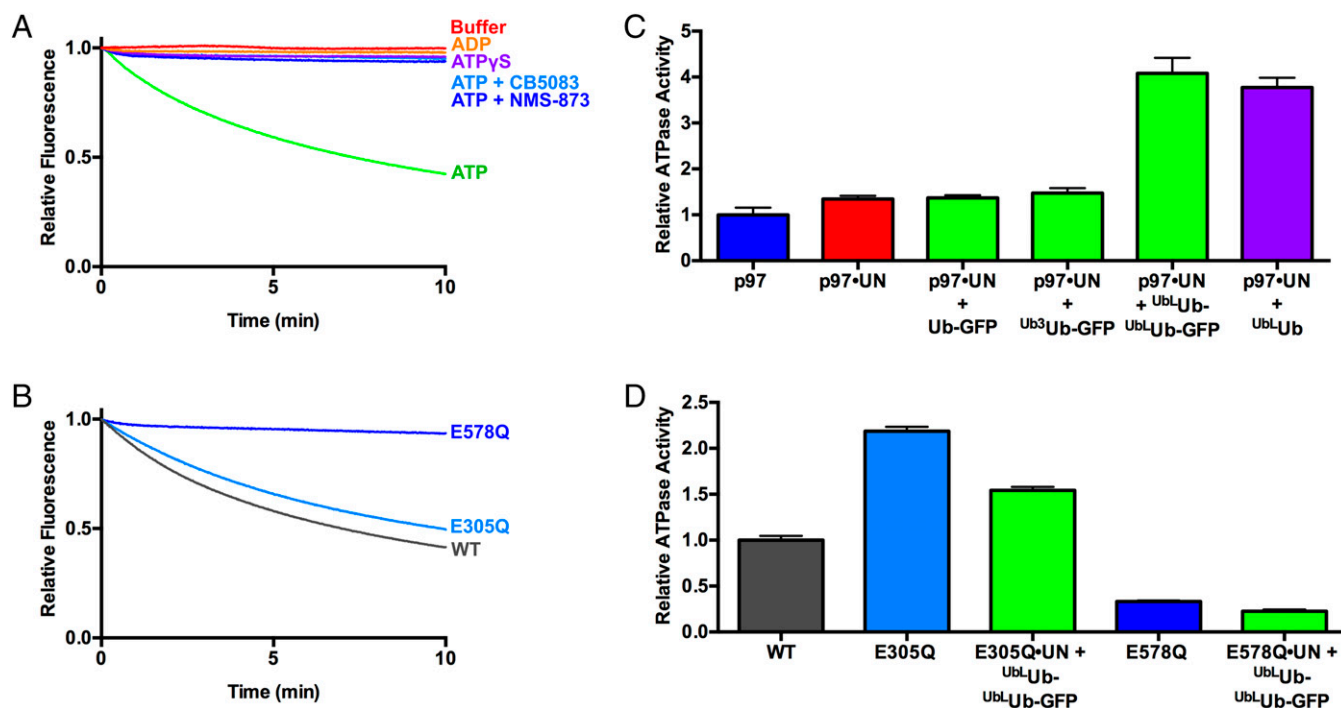


Fig. 4. ATPase activity of p97 is critical for and stimulated by substrate unfolding. (A) Fluorescence traces of $U^{bL}Ub-U^{bL}Ub-GFP$ in the presence of p97, UN, GroEL, and various nucleotides and p97 inhibitors. Unfolding was observed only in the presence of ATP. Representative traces shown ($n \geq 2$). (B) Unfolding of $U^{bL}Ub-U^{bL}Ub-GFP$ by p97 ATPase mutants. p97-E305Q and p97-E578Q are deficient in D1 and D2 ATPase activity, respectively. p97-E305Q was able to unfold substrate, whereas p97-E578Q was not. Representative traces shown ($n \geq 3$). (C) Substrate stimulates ATPase activity of p97 when UN is present. Unanchored ubiquitin chains and those linked to Ub-GFP yielded equivalent stimulation, whereas Ub-GFP and $U^{b3}Ub-GFP$ did not stimulate. ATPase activity was measured with BIOMOL Green as described in *Methods* and was normalized to basal WT p97 activity. Error bars represent SD ($n = 4$). (D) Effect of substrate plus UN on ATPase activity of D1 and D2 domain ATPase mutants. Addition of $U^{bL}Ub-U^{bL}Ub-GFP$ plus UN slightly decreased ATPase activities of D1 mutant E305Q and D2 mutant E578Q. Error bars represent SD ($n = 4$).

Table 1. Rates and extents of unfolding of ^{UbL}Ub-^{UbL}Ub-GFP by p97 mutants

Mutant	Rate, s ⁻¹	Plateau, %	n
WT	0.195 ± 0.007	33.3 ± 0.8	6
E305Q	0.154 ± 0.005	36.5 ± 0.8	3
E578Q	ND	ND	3
A232E	0.274 ± 0.007	25.3 ± 0.4	3

The rates and plateaus were calculated by fitting data to a single exponential decay, with the plateau representing the percentage of fluorescence remaining at the end of the reaction. Unpaired *t* tests comparing WT rates vs. those of p97-E305Q and p97-A232E yielded *P* values of <0.0001 in both cases, indicating statistically significant differences. Sample size represents number of technical replicates, and values are shown ± SD. ND, not detected.

binding to our beads even in the absence of antibody (Fig. 5A, lane 1). The binding signal was increased in lanes 6 and 7 (Fig. 5A), but this could be the result of p97, which, in our experience, is prone to exhibit nonspecific binding.

Whereas the unfolding of substrate was highly dependent on ATP hydrolysis, substrate interaction with p97 was not. IP of FLAG-Ub^LUb^L-FLAG-Ub^LUb-GFP pulled down equal amounts of p97 in the absence of added nucleotide and in the presence of ATP, ATPγS, ATP plus NMS-873, and ATP plus CB-5083 (Fig. 5C). Therefore, p97 does not have to be actively remodeling substrate to effectively form a tight complex. Loss of binding of p97, but not UN, was seen only with added ADP, which could be the result of the large conformational changes observed for p97 in its ADP-bound state (18) (Fig. 5C). These results are consistent with previous studies on Ub chain association with p97 and p97•UN (48, 82).

IBMPFD Mutant p97-A232E Has Enhanced Unfoldase Activity. The autosomal-dominant human syndrome IBMPFD is caused by mutations that cluster at the interface of the N and D1 domains of p97. Of the different IBMPFD mutations that have been identified in p97, A232E exhibits the most severe phenotype in terms of age of onset and penetrance. In addition, p97-A232E consistently shows higher basal D2 ATPase rates than WT enzyme (20, 63, 65). The availability of an assay that directly measures ATP-dependent unfolding by p97 allowed us to distinguish between two alternative interpretations of the significance of the enhanced ATPase activity of the A232E mutant protein. The enhanced activity may reflect a true gain of function wherein p97-A232E is a more powerful or faster motor. On the contrary, ATPase activity may increase because of decoupling of the D2 “motor” from the substrate “load,” analogous to pushing in the clutch when an engine is revving in low gear. If the former is more accurate, we would expect to see increased unfolding by the mutant protein. Conversely, if the latter is correct, we would expect to see reduced unfolding. The result of this experiment was unambiguous: p97-A232E exhibited accelerated unfolding of GFP under the single-turnover conditions used in the assay (Fig. 6A and Table 1). This effect is reproducible, because, in two independent sets of preparations, p97-A232E displayed faster unfolding than WT p97 (Fig. 6A and C). The substrate-induced ATPase acceleration observed for WT p97 was also observed with p97-A232E (Fig. 6B). The mutant protein displays an increased basal rate of ATP hydrolysis and a higher rate in the presence of substrate compared with WT.

We identified a reversible, ATP-competitive p97 ATPase inhibitor that was recently perfected to yield the clinical candidate CB-5083 (81), which is in human phase I clinical trials for treatment of cancer. If the basis of IBMPFD pathology is the result of enhanced unfoldase activity of p97, we reasoned that CB-5083 could potentially be explored as a therapy for IBMPFD. To test the feasibility of this idea, we performed unfolding reactions with p97-A232E at several different concentrations of CB-5083.

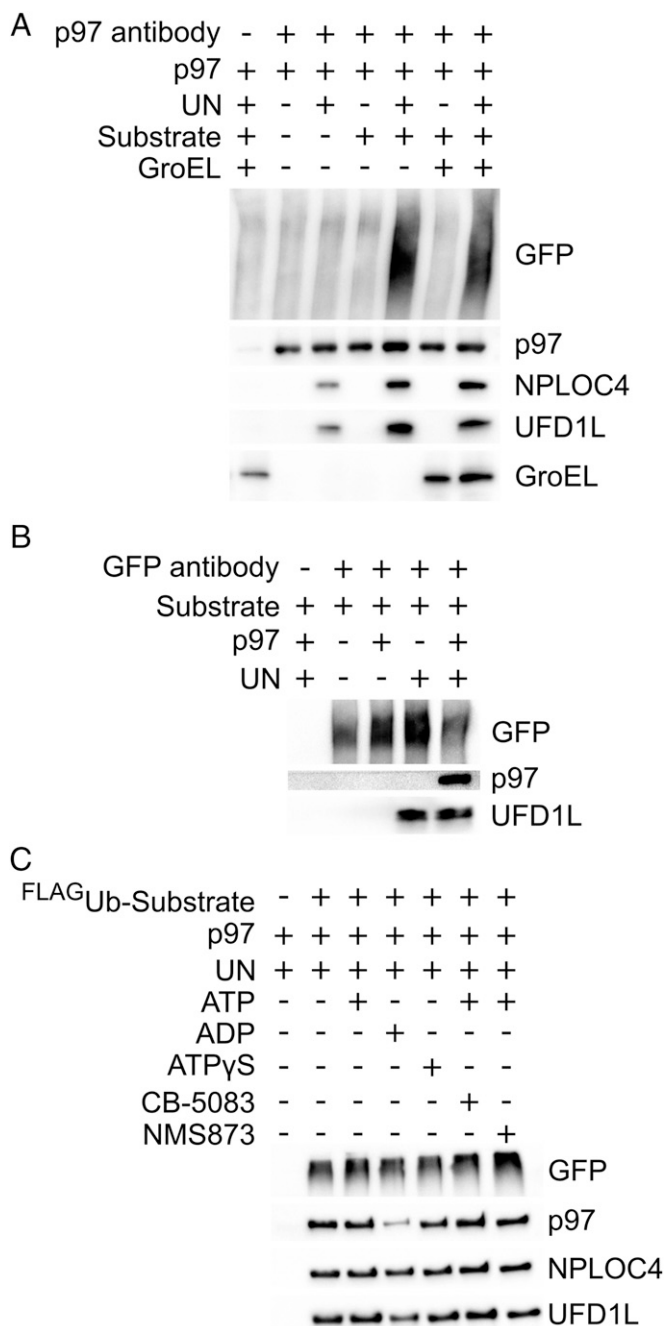


Fig. 5. UN recruits ubiquitylated substrate to p97. (A) Association of substrate with p97 depends on UN. Reactions containing 100 nM p97, 200 nM UN, 200 nM ^{UbL}Ub-^{UbL}Ub-GFP, and/or 200 nM GroEL were immunoprecipitated by using an anti-p97 antibody and assessed by Western blot. Substrate was pulled down with p97 only in the presence of UN, and substrate enhanced the binding of UN to p97. Effects of substrate and UN on binding of GroEL to p97 could not be determined as a result of high background binding of GroEL to beads, antibody, and/or p97. (B) UN binds directly to substrate and links it to p97. Samples prepared as in A were immunoprecipitated with an anti-GFP antibody. Substrate pulled down UN but bound p97 only in the presence of UN. (C) Bound nucleotide has only a modest effect on formation of a p97•UN•substrate ternary complex. Samples prepared as in A with various nucleotides and/or p97 inhibitors were immunoprecipitated by anti-FLAG resin, which bound the FLAG-tagged ubiquitin on substrate. Binding of p97, but not UN, was reduced only in the ADP state.

Remarkably, when added at 37.5 nM, or one molecule per two p97 hexamers, CB-5083 normalized the unfolding rate of p97-A232E to match that of WT (Fig. 6C).

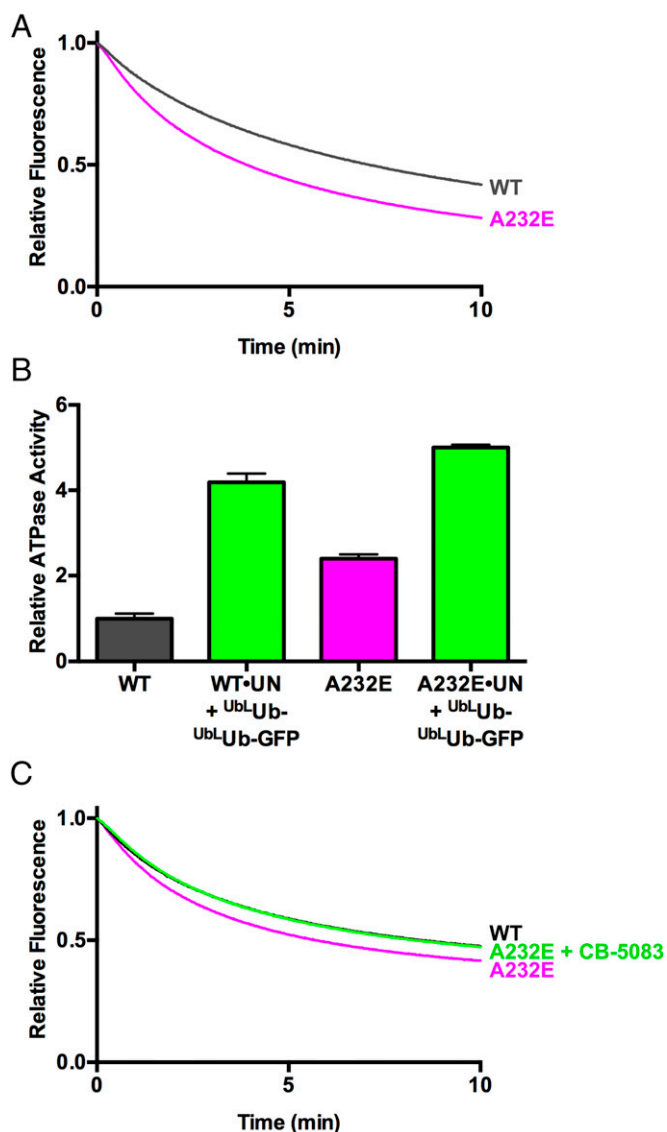


Fig. 6. IMBPF mutant p97-A232E is a better unfoldase. (A) In the presence of UN and GroEL, p97-A232E catalyzed the loss of fluorescence of $^{UbL}Ub-^{UbL}Ub-GFP$ faster than WT, suggesting it acts as an improved unfoldase. Rates are listed in Table 1, and the difference between WT and p97-A232E is statistically significant at $P < 0.0001$. Representative traces shown ($n \geq 3$). (B) p97-A232E shows accelerated ATPase rates in the presence of UN and substrate. The IMBPF mutant also had a higher baseline ATPase rate than WT (unpaired t test, $P < 0.0001$) and a higher ATPase activity in the presence of UN and substrate compared with WT (unpaired t test, $P = 0.0003$). ATPase activity was measured with BIOMOL Green as described in *Methods* and was normalized to basal WT p97 activity. Error bars represent SD ($n = 4$). (C) Addition of a 37.5-nM CB-5083 restores p97-A232E unfoldase activity to WT levels. Representative traces shown ($n = 2$), and the difference between WT and p97-A232E rates is statistically significant (unpaired t test, $P = 0.02$). Independent preparations of proteins were used for A and C.

Discussion

P97/VCP is implicated in a broad range of cellular processes including membrane fusion, protein trafficking, and ubiquitin-dependent proteolysis (1). It is thought that the core biochemical activity of p97 that enables its diverse biological functions is its ability to act as a segregase that segregates polypeptides from binding partners in multisubunit complexes, or from large macromolecular structures including ribosomes, membranes, or chromatin. Although the mechanism by which p97 exerts segregase activity is not known,

the most economical hypothesis is that it grabs onto the polypeptide to be segregated and commences to unfold it. However, despite the appeal of this unifying hypothesis, the ability of WT p97 to harvest the energy of ATP hydrolysis to unfold a polypeptide has never been directly demonstrated. We show here, in a well-defined system, that WT p97 can at least partially unfold a protein. In contrast to prior studies that used a doubly mutated p97 acting upon an unmodified protein in the absence of any adaptor (83, 84), the unfolding we observe exhibits dependencies predicted from prior genetic and biochemical studies of p97, including dependence on ATP hydrolysis by the D2 ATPase domain of p97, the heterodimeric adaptor NPLOC4•UFD1L, and conjugation of an ubiquitin chain to the substrate that is unfolded (1, 24, 25).

Despite the close alignment of *in vitro* dependencies reported here with known *in vivo* requirements for p97 action, there are two caveats worth noting. First, we do not know whether the loss of GFP fluorescence is the result of complete unfolding or local unfolding. Second, our Ub-GFP model substrate is not a native substrate of p97. However, p97 activity in the UFD pathway is absolutely required for its degradation *in vivo* in yeast, *Drosophila*, and human cells (19, 47, 70, 72), and the E2–E3 chimera used to ubiquitylate Ub-GFP was derived from enzymes that function directly upstream of p97 in the ERAD pathway (73). Thus, we believe the reaction reported here represents the essence of p97's biochemical activity that underlies its physiological functions.

Processing of our Ub-GFP substrate by p97 is dependent on the conjugation of multiple ubiquitins connected by K48 linkages, which is consistent with reports of K48-linked ubiquitin chain binding by p97 and UFD1L and linkage-nonspecific chain binding by NPLOC4 (25, 48, 49, 82). One of our most interesting findings is that we observed enhanced substrate unfolding when the substrate contained a branch point enabling the formation of multiple K48-linked ubiquitin chains. Our substrate contains a branch at the base of the ubiquitin conjugate, which allows for two K48-linked chains to be built on a single site of substrate modification. Because there are multiple ubiquitin binding sites on the p97•UN complex, the branched chain on our $^{UbL}Ub-^{UbL}Ub-GFP$ substrate may retard, via enhanced avidity, its dissociation before unfolding. Branched ubiquitin chains can enhance substrate degradation (85) and have been associated with p97 previously. Ubiquitin chains with K11 linkages are associated with ERAD (86). Substrates modified with K11 and K11–K48 branched chains associate with p97•UN and its *Drosophila* ortholog (87, 88), and p97 binds K11–K48 branched chains better than either type of homotypic chain (85). Furthermore, K29 and K48 linkages are formed on UFD pathway substrates *in vivo* and *in vitro* using purified UFD pathway enzymes (47, 89). Whereas our data with linear ubiquitin fusions suggest that branched and/or multiple ubiquitin chains may be important for interaction of substrates with p97•UN, further work with physiological linkages *in vitro* and *in vivo* is needed to determine the exact requirements for ubiquitylated p97 substrates.

The second requirement for p97-catalyzed unfolding is the heterodimeric adaptor UN. In agreement with prior work, UN bridges the interaction of substrates with p97 (25, 48). However, p97 also associates with other adaptor proteins, some of which (e.g., UBXN7) can cobind with UN and others (e.g., NSFL1C) of which bind in a mutually exclusive manner (36, 37, 46, 90, 91). Although there are examples of processes that require UN and an additional adaptor (42, 92), in general, it is unclear whether the different adaptors work in different pathways, or work sequentially, together, or in opposition to one another in the same pathway. Mutually exclusive adaptors like NSFL1C bind very differently from UN yet also promote protein segregation (41, 51, 93). However, neither NSFL1C nor UBXN7 was able to replace UN in our unfolding assay, suggesting that they promote substrate processing in a different way or work on different

substrates. Our assay provides a platform for further mechanistic exploration of the functional relationship between different adaptor proteins.

The final requirement for unfolding of GFP is ATP hydrolysis by the D2 ATPase of p97. Our results are in direct contrast with a previous study that showed that p97-dependent unfolding is inhibited by ATP (94), but are consistent with overwhelming *in vitro* and *in vivo* data (1, 23, 25, 34). Our experiments with p97 mutants and the D2-specific ATP-competitive inhibitor CB-5083 demonstrate the importance of D2 ATPase activity over that of D1, which confirms prior observations (19–25). We observed very little effect of the D1 Walker B mutant on substrate processing, leaving the role of D1 ATPase activity in p97 function unclear (1). Not only is the ATPase activity key to substrate processing, but we also observed its stimulation by ubiquitin chain or substrate binding. This stimulation was abolished in the D1 Walker B mutant. Nevertheless, this mutant unfolded GFP at near-WT rates, suggesting that substrate stimulation of ATP hydrolysis might not be essential, at least for some substrates. ATPase acceleration in the presence of the cytoplasmic fragment of the ERAD substrate Sytl has been previously reported, but, unlike the stimulation reported here, it was not dependent on UN or ubiquitylation of the substrate (34), both of which are thought to be requirements for ERAD. p97 can interact with a substrate and the ubiquitin chain appended to the substrate (25, 95), suggesting that stimulation of p97 ATPase and perhaps substrate processing can be regulated through multiple binding interfaces. Even though we are unable to draw any conclusions about the mechanism of unfolding by p97, studies on the archaeobacterial homolog VAT support a model whereby substrate is translocated through the central channel (14, 15), suggesting that adaptor and substrate engagement must expand p97's narrow pore (16, 18) to accommodate the threading of an unfolded polypeptide chain.

Mutations in p97 cause the autosomal-dominant human disease IBMPFD (53). Prior work has led to conflicting proposals regarding the underlying basis for pathogenesis in IBMPFD. Some studies have emphasized a reduction in specific biological functions of the mutant p97, including its roles in endosomal trafficking, autophagy, and elimination of leaky lysosomes (8, 56, 60). Defects in these processes have been linked to reduced binding of mutant p97 to UBXD1 (8). On the contrary, IBMPFD mutant proteins hydrolyze ATP at a faster rate (20, 63–65). Whereas it has been speculated that the increase in ATP hydrolysis might be the result of an uncoupling of substrate binding via the N domain to mechanochemical transduction in the D2 domain (54, 68), studies in *Drosophila* point to an increase in function for the mutant p97 (61, 67, 69). Furthermore, the overexpression of WT p97 enhanced IBMPFD mutant phenotypes whereas inactivation of one copy of WT p97 suppressed mutant phenotypes, which is consistent with a gain-of-function mutation (96). The availability of a biochemical assay that directly measures substrate unfolding, which we propose is the core biochemical activity underlying p97's myriad biological functions, allowed us to investigate this issue. We focused on the mutant with the most severe disease phenotype, p97-A232E, and observed a modest but reproducible increase in the rate of substrate unfolding that was renormalized by addition of an ATP-competitive inhibitor, implying that the underlying defect in this disease may result in part from a true gain of function rather than the prevailing loss-of-function hypothesis. Our results call to mind previous work to engineer Hsp104, in which point mutations greatly augmented its ATPase and unfoldase activity while altering intersubunit communication (97). It is interesting that the increased ATPase activity of p97-E305Q did not cause a similar increase in unfolding rate, suggesting that the rate of ATP hydrolysis in D2 does not by itself determine the rate of unfolding. Our experiments were carried out with pure WT and pure mutant p97, so it will be of interest to study populations of mixed hexamers of A232E and other IBMPFD

mutants to better recapitulate the situation that pertains *in vivo*. Whereas much clearly remains to be done to further investigate this gain-of-function model, if our proposal is correct, it implies that the clinical-grade p97 inhibitor (81) that renormalized the activity of the mutant protein may be useful for therapy of IBMPFD and ALS cases that arise from mutation of p97.

Methods

A description of previously published proteins used in this study can be found in Table S1.

gp78RING-Ube2g2 Chimera Construction and Purification. A 72-residue sequence of the E3 ubiquitin protein ligase gp78/AMFR (residues 322–393), containing the RING domain, was fused to the N terminus of the ubiquitin-conjugating enzyme Ube2g2 with a linker sequence of GTGSH. cDNA encoding this fusion protein was inserted into the bacterial expression plasmid p28a-TEV vector to encode a polyHis-tagged protein. Protein was expressed in BL21(DE3) at 37 °C with 0.4 mM IPTG for 4 h and was purified on Ni-NTA resin and a Superdex 75 column before being cleaved with TEV protease overnight at 4 °C. Cleaved protein was then bound to a MonoQ ion exchange column, eluted with a NaCl gradient (0.05–0.5 M), concentrated with centrifugal filter units, and flash-frozen.

Ub^{G76V}GFP Fusion Construction. The coding sequence for Ub^{G76V}GFP in the EGFP-N1 vector Raymond Deshaies bacteria (RDB) no. 1832] (19) was PCR-amplified and inserted into pET28a by using NdeI and NotI sites to produce His₆-Ub^{G76V}-GFP (RDB no. 3006). His₆-Ub^{G76V}-Ub^{G76V}-GFP (RDB no. 3344) and His₆-Ub^{G76V}-Ub^{G76V}-Ub^{G76V}-GFP (RDB no. 3345) were created by ligating Ub₂^{G76V} and Ub₃^{G76V}, PCR-amplified from a synthetic Ub₄^{G76V} sequence (RDB no. 2406), into His-Ub^{G76V}-GFP cut with NdeI and HindIII. For simplification, the G76V notation has been left out of subsequent mentions of these constructs.

Ub³Ub-GFP Synthesis and Purification. A plasmid for bacterial expression of Ub-K48R (RDB no. 3348) was made from that of Ub (RDB no. 2805) by site-directed mutagenesis, and the protein was expressed as previously described (76). Pure K48-linked Ub₃ chains carrying a K48R mutation in the distal Ub were enzymatically synthesized and purified as described previously (76, 77). To form Ub³Ub-GFP, 0.5 μM Ube1 (E1), 5 μM gp78RING-Ube2g2, 2.5 μM Ub-GFP, and 5 μM Ub₃ were incubated in 20 mM HEPES, pH 7.4, 5 mM ATP, and 5 mM MgCl₂ overnight at 37 °C. The Ub³Ub-GFP was then purified on Ni-NTA resin and a Superdex 200 gel filtration column before being concentrated with centrifugal filter units and flash-frozen.

Polyubiquitylated Substrate Synthesis and Purification. Reactions were carried out with final concentrations of 10 μM Ub-GFP fusion protein, 1 μM E1, 20 μM gp78RING-Ube2g2, and 400 μM ubiquitin in 20 mM HEPES, pH 7.4, 10 mM ATP, and 10 mM MgCl₂ at 37 °C overnight. Ubiquitin was added progressively in small amounts over the first 8 h of the reaction. For FLAG-tagged substrate, 40 μM FLAG-Ubiquitin (Boston Biochem) was added in the first 2 h. To purify ubiquitylated GFP from free ubiquitin chains, the reaction mixture was incubated with Ni-NTA resin, eluted with 300 mM imidazole, and run over a Superose 6 size-exclusion column in 20 mM HEPES, pH 7.4, 250 mM KCl, 1 mM MgCl₂, 1 mM tris(2-carboxyethyl)phosphine (TCEP), and 5% glycerol. Fractions were pooled into long, medium, and short chain-length samples, concentrated with centrifugal filter units, and flash-frozen.

ATPase Assays. The ATPase assay protocol was modified from previously published methods (40). In an untreated microplate (no. 655101; Greiner Bio-One), 40-μL solutions containing 30 nM p97 hexamer, 150 nM adaptor, and/or 150 nM substrate in ATPase assay buffer (25 mM HEPES, pH 7.4, 100 mM KCl, 3 mM MgCl₂, 1 mM TCEP, 0.1 mg/mL ovalbumin) were preincubated at 37 °C for 10 min. To this, 10 μL of a 1-mM ATP solution was added, and the reaction was incubated at 37 °C for 5 or 10 min. After cooling on ice for 30 s, 50 μL of BIOMOL Green reagent (Enzo Life Sciences) was added. Solutions were developed at room temperature for 30 min before being read at 600 nm. The amount of inorganic phosphate in each sample was calculated from a standard curve, and relative ATPase activity for a sample was calculated by normalizing its measurement to that of samples of WT p97 alone.

Fluorescence Unfolding Assays. Unless specified, all assays were carried out at 37 °C. Samples contained 25 nM GFP substrate, 75 nM p97 hexamer, 150 nM adaptor (UN, NSFL1C, or UBXN7), and/or 250 nM GroEL trap in unfolding assay buffer (25 mM HEPES, pH 7.4, 100 mM KCl, 5 mM MgCl₂, 1 mM TCEP, 2 mM ATP). Control experiments indicated that the levels of p97, adaptor, and GroEL used

were at or near saturation (Fig. 2 and Fig. S5). Other nucleotides and p97 inhibitors were present at 2 mM and 10 μ M, respectively, when indicated. Kinetic experiments were carried out on a Fluoro-Log 3 (Horiba Jobin Yvon) with excitation at 488 nm and emission at 509 nm. Relative fluorescence was calculated by normalizing the fluorescence signal to that at time 0. Unfolding rates were calculated by fitting curves to an exponential decay model in Prism (GraphPad).

Binding Assays. Antibodies used for IP and Western blotting are listed in Table S2. Samples containing 100 nM p97, 200 nM UN, 200 nM GFP substrate, and/or 200 nM GroEL trap in binding assay buffer (25 mM Hepes, pH 7.4, 100 mM KCl, 3 mM MgCl₂, 1 mM TCEP) in a volume of 200 μ L were preincubated at 37 °C for 15 min. Triton X-100 interfered with binding of substrate to GroEL trap, so 0.01% Triton X-100 was included in all buffers only in reactions that did not contain GroEL. Nucleotides and inhibitors were present at 2 mM and 10 μ M, respectively, where indicated. For IPs that used Protein G magnetic beads (Bio-Rad Laboratories), protein mixtures were incubated with 1 μ L of

antibody for 15 min at 37 °C before a 1-h incubation with 25 μ L of beads at room temperature. For FLAG IPs, reactions were incubated with 25 μ L of anti-FLAG resin (Sigma-Aldrich) for 15 min at room temperature. Following incubation, all beads were washed three times with 750 μ L assay buffer before being boiled in 50 μ L 2 \times SDS/PAGE loading dye. Samples were then analyzed by Western blot.

ACKNOWLEDGMENTS. We thank Willem den Besten, David Sherman, and Jing Li for assistance with cloning and protein purification; Arthur Horwich for the GroEL expression plasmid and antibody; Rati Verma and David Sherman for comments on the manuscript; the entire laboratory of R.J.D. for helpful discussion; and Tom Rapoport for communicating results before publication. Fluorescence measurements were carried out in the Beckman Institute Laser Resource Center and the Caltech Biophysical Facility. R.J.D. is an Investigator of the Howard Hughes Medical Institute (HHMI), and this work was supported by HHMI.

- Chapman E, Fry AN, Kang M (2011) The complexities of p97 function in health and disease. *Mol Biosyst* 7:700–710.
- Wang Q, Song C, Li C-CH (2004) Molecular perspectives on p97-VCP: Progress in understanding its structure and diverse biological functions. *J Struct Biol* 146:44–57.
- Wolf DH, Stolz A (2012) The Cdc48 machine in endoplasmic reticulum associated protein degradation. *Biochim Biophys Acta* 1823:117–124.
- Verma R, Oania RS, Kolawa NJ, Deshaies RJ (2013) Cdc48/p97 promotes degradation of aberrant nascent polypeptides bound to the ribosome. *eLife* 2:e00308.
- Xu S, Peng G, Wang Y, Fang S, Karbowski M (2011) The AAA-ATPase p97 is essential for outer mitochondrial membrane protein turnover. *Mol Biol Cell* 22:291–300.
- Defenouillere Q, et al. (2013) Cdc48-associated complex bound to 60S particles is required for the clearance of aberrant translation products. *Proc Natl Acad Sci USA* 110:5046–5051.
- Rabouille C, Levine TP, Peters J-M, Warren G (1995) An NSF-like ATPase, p97, and NSF mediate cristernal regrowth from mitotic Golgi fragments. *Cell* 82:905–914.
- Ritz D, et al. (2011) Endolysosomal sorting of ubiquitylated caveolin-1 is regulated by VCP and UBXD1 and impaired by VCP disease mutations. *Nat Cell Biol* 13:1116–1123.
- Ye Y (2006) Diverse functions with a common regulator: Ubiquitin takes command of an AAA ATPase. *J Struct Biol* 156:29–40.
- Meyer H, Bug M, Bremer S (2012) Emerging functions of the VCP/p97 AAA-ATPase in the ubiquitin system. *Nat Cell Biol* 14:117–123.
- Förster F, Schuller JM, Unverdorben P, Aufderheide A (2014) Emerging mechanistic insights into AAA complexes regulating proteasomal degradation. *Biomolecules* 4: 774–794.
- Liu CW, et al. (2002) Conformational remodeling of proteasomal substrates by PA700, the 19 S regulatory complex of the 26 S proteasome. *J Biol Chem* 277: 26815–26820.
- Weber-Ban EU, Reid BG, Miranker AD, Horwich AL (1999) Global unfolding of a substrate protein by the Hsp100 chaperone ClpA. *Nature* 401:90–93.
- Gerega A, et al. (2005) VAT, the thermoplasma homolog of mammalian p97/VCP, is an N domain-regulated protein unfoldase. *J Biol Chem* 280:42856–42862.
- Barthelme D, Sauer RT (2012) Identification of the Cdc48•20S proteasome as an ancient AAA+ proteolytic machine. *Science* 337:843–846.
- DeLaBarre B, Brunger AT (2005) Nucleotide dependent motion and mechanism of action of p97/VCP. *J Mol Biol* 347:437–452.
- Hänzelmann P, Schindelin H (2016) Structural basis of ATP hydrolysis and inter-subunit signaling in the AAA+ ATPase p97. *Structure* 24:127–139.
- Banerjee S, et al. (2016) 2.3 Å resolution cryo-EM structure of human p97 and mechanism of allosteric inhibition. *Science* 351:871–875.
- Beskow A, et al. (2009) A conserved unfoldase activity for the p97 AAA-ATPase in proteasomal degradation. *J Mol Biol* 394:732–746.
- Chou T-F, et al. (2014) Specific inhibition of p97/VCP ATPase and kinetic analysis demonstrate interaction between D1 and D2 ATPase domains. *J Mol Biol* 426: 2886–2899.
- Wang Q, Song C, Li C-CH (2003) Hexamerization of p97-VCP is promoted by ATP binding to the D1 domain and required for ATPase and biological activities. *Biochem Biophys Res Commun* 300:253–260.
- Briggs LC, et al. (2008) Analysis of nucleotide binding to P97 reveals the properties of a tandem AAA hexameric ATPase. *J Biol Chem* 283:13745–13752.
- Esaki M, Ogura T (2010) ATP-bound form of the D1 AAA domain inhibits an essential function of Cdc48p/p97. *Biochem Cell Biol* 88:109–117.
- Song C, Wang Q, Li CC (2003) ATPase activity of p97-valosin-containing protein (VCP). D2 mediates the major enzyme activity, and D1 contributes to the heat-induced activity. *J Biol Chem* 278:3648–3655.
- Ye Y, Meyer HH, Rapoport TA (2003) Function of the p97-Ufd1-Npl4 complex in retrotranslocation from the ER to the cytosol: Dual recognition of nonubiquitinated polypeptide segments and polyubiquitin chains. *J Cell Biol* 162:71–84.
- Davies JM, Brunger AT, Weis WI (2008) Improved structures of full-length p97, an AAA ATPase: Implications for mechanisms of nucleotide-dependent conformational change. *Structure* 16:715–726.
- Nishikori S, Esaki M, Yamanaka K, Sugimoto S, Ogura T (2011) Positive cooperativity of the p97 AAA ATPase is critical for essential functions. *J Biol Chem* 286: 15815–15820.
- Li G, Huang C, Zhao G, Lennarz WJ (2012) Interprotomer motion-transmission mechanism for the hexameric AAA ATPase p97. *Proc Natl Acad Sci USA* 109: 3737–3741.
- Yeung HO, et al. (2014) Inter-ring rotations of AAA ATPase p97 revealed by electron cryomicroscopy. *Open Biol* 4:130142.
- Schuller JM, Beck F, Lössl P, Heck AJR, Förster F (2016) Nucleotide-dependent conformational changes of the AAA+ ATPase p97 revisited. *FEBS Lett* 590:595–604.
- Tang WK, Xia D (2016) Role of the D1-D2 linker of human VCP/p97 in the asymmetry and ATPase activity of the D1-domain. *Sci Rep* 6:20037.
- Rouiller I, et al. (2002) Conformational changes of the multifunction p97 AAA ATPase during its ATPase cycle. *Nat Struct Biol* 9:950–957.
- Hinnerwisch J, Fenton WA, Furtak KJ, Farr GW, Horwich AL (2005) Loops in the central channel of ClpA chaperone mediate protein binding, unfolding, and translocation. *Cell* 121:1029–1041.
- DeLaBarre B, Christianson JC, Kopito RR, Brunger AT (2006) Central pore residues mediate the p97/VCP activity required for ERAD. *Mol Cell* 22:451–462.
- Zhao M, et al. (2015) Mechanistic insights into the recycling machine of the SNARE complex. *Nature* 518:61–67.
- Schuberth C, Buchberger A (2008) UBX domain proteins: Major regulators of the AAA ATPase Cdc48/p97. *Cell Mol Life Sci* 65:2360–2371.
- Alexandru G, et al. (2008) UBXD7 binds multiple ubiquitin ligases and implicates p97 in HIF1 α turnover. *Cell* 134:804–816.
- Meyer HH, Kondo H, Warren G (1998) The p47 co-factor regulates the ATPase activity of the membrane fusion protein, p97. *FEBS Lett* 437:255–257.
- Bruderer RM, Brasseur C, Meyer HH (2004) The AAA ATPase p97/VCP interacts with its alternative co-factors, Ufd1-Npl4 and p47, through a common bipartite binding mechanism. *J Biol Chem* 279:49609–49616.
- Zhang X, et al. (2015) Altered cofactor regulation with disease-associated p97/VCP mutations. *Proc Natl Acad Sci USA* 112:E1705–E1714.
- Kondo H, et al. (1997) p47 is a cofactor for p97-mediated membrane fusion. *Nature* 388:75–78.
- Verma R, Oania R, Fang R, Smith GT, Deshaies RJ (2011) Cdc48/p97 mediates UV-dependent turnover of RNA Pol II. *Mol Cell* 41:82–92.
- den Besten W, Verma R, Kleiger G, Oania RS, Deshaies RJ (2012) NEDD8 links cullin-RING ubiquitin ligase function to the p97 pathway. *Nat Struct Mol Biol* 19:511–516, S1.
- Raman M, et al. (2015) Systematic proteomics of the VCP-UBXD adaptor network identifies a role for UBXN10 in regulating ciliogenesis. *Nat Cell Biol* 17:1356–1369.
- Bays NW, Wilhovskiy SK, Goradia A, Hodgkiss-Harlow K, Hampton RY (2001) HRD4/NPL4 is required for the proteasomal processing of ubiquitinated ER proteins. *Mol Biol Cell* 12:4114–4128.
- Meyer HH, Shorter JG, Seemann J, Pappin D, Warren G (2000) A complex of mammalian ufd1 and npl4 links the AAA-ATPase, p97, to ubiquitin and nuclear transport pathways. *EMBO J* 19:2181–2192.
- Johnson ES, Ma PC, Ota IM, Varshavsky A (1995) A proteolytic pathway that recognizes ubiquitin as a degradation signal. *J Biol Chem* 270:17442–17456.
- Meyer HH, Wang Y, Warren G (2002) Direct binding of ubiquitin conjugates by the mammalian p97 adaptor complexes, p47 and Ufd1-Npl4. *EMBO J* 21:5645–5652.
- Pye VE, et al. (2007) Structural insights into the p97-Ufd1-Npl4 complex. *Proc Natl Acad Sci USA* 104:467–472.
- Isaacson RL, et al. (2007) Detailed structural insights into the p97-Npl4-Ufd1 interface. *J Biol Chem* 282:21361–21369.
- Bebeacua C, et al. (2012) Distinct conformations of the protein complex p97-Ufd1-Npl4 revealed by electron cryomicroscopy. *Proc Natl Acad Sci USA* 109:1098–1103.
- Hänzelmann P, Schindelin H (2016) Characterization of an additional binding surface on the p97 N-terminal domain involved in bipartite cofactor interactions. *Structure* 24:140–147.
- Watts GDJ, et al. (2004) Inclusion body myopathy associated with Paget disease of bone and frontotemporal dementia is caused by mutant valosin-containing protein. *Nat Genet* 36:377–381.
- Tang WK, Xia D (2016) Mutations in the human AAA(+) chaperone p97 and related diseases. *Front Mol Biosci* 3:79.
- Johnson JO, et al.; ITALSGEN Consortium (2010) Exome sequencing reveals VCP mutations as a cause of familial ALS. *Neuron* 68:857–864.

56. Ju J-S, et al. (2009) Valosin-containing protein (VCP) is required for autophagy and is disrupted in VCP disease. *J Cell Biol* 187:875–888.
57. Tresse E, et al. (2010) VCP/p97 is essential for maturation of ubiquitin-containing autophagosomes and this function is impaired by mutations that cause IBMPPD. *Autophagy* 6:217–227.
58. Ramanathan HN, Ye Y (2012) The p97 ATPase associates with EEA1 to regulate the size of early endosomes. *Cell Res* 22:346–359.
59. Ching JK, et al. (2013) mTOR dysfunction contributes to vacuolar pathology and weakness in valosin-containing protein associated inclusion body myopathy. *Hum Mol Genet* 22:1167–1179.
60. Papadopoulos C, et al. (2017) VCP/p97 cooperates with YOD1, UBXD1 and PLAA to drive clearance of ruptured lysosomes by autophagy. *EMBO J* 36:135–150.
61. Zhang T, Mishra P, Hay BA, Chan D, Guo M (2017) Valosin-containing protein (VCP/p97) inhibitors relieve Mitofusins-dependent mitochondrial defects due to VCP disease mutants. *eLife* 6:e17834.
62. Fernández-Sáiz V, Buchberger A (2010) Imbalances in p97 co-factor interactions in human proteinopathy. *EMBO Rep* 11:479–485.
63. Niwa H, et al. (2012) The role of the N-domain in the ATPase activity of the mammalian AAA ATPase p97/VCP. *J Biol Chem* 287:8561–8570.
64. Halawani D, et al. (2009) Hereditary inclusion body myopathy-linked p97/VCP mutations in the NH2 domain and the D1 ring modulate p97/VCP ATPase activity and D2 ring conformation. *Mol Cell Biol* 29:4484–4494.
65. Tang WK, Xia D (2013) Altered intersubunit communication is the molecular basis for functional defects of pathogenic p97 mutants. *J Biol Chem* 288:36624–36635.
66. Tang WK, et al. (2010) A novel ATP-dependent conformation in p97 N-D1 fragment revealed by crystal structures of disease-related mutants. *EMBO J* 29:2217–2229.
67. Manno A, Noguchi M, Fukushi J, Motohashi Y, Kakizuka A (2010) Enhanced ATPase activities as a primary defect of mutant valosin-containing proteins that cause inclusion body myopathy associated with Paget disease of bone and frontotemporal dementia: Enhanced ATPase activities in IBMPPD-VCPs. *Genes Cells* 15:911–922.
68. Ju JS, Weihl CC (2010) Inclusion body myopathy, Paget's disease of the bone and fronto-temporal dementia: A disorder of autophagy. *Hum Mol Genet* 19:R38–R45.
69. Ritson GP, et al. (2010) TDP-43 mediates degeneration in a novel *Drosophila* model of disease caused by mutations in VCP/p97. *J Neurosci* 30:7729–7739.
70. Johnson ES, Bartel B, Seufert W, Varshavsky A (1992) Ubiquitin as a degradation signal. *EMBO J* 11:497–505.
71. Bachmair A, Finley D, Varshavsky A (1986) In vivo half-life of a protein is a function of its amino-terminal residue. *Science* 234:179–186.
72. Wójcik C, et al. (2006) Valosin-containing protein (p97) is a regulator of endoplasmic reticulum stress and of the degradation of N-end rule and ubiquitin-fusion degradation pathway substrates in mammalian cells. *Mol Biol Cell* 17:4606–4618.
73. Ballar P, Shen Y, Yang H, Fang S (2006) The role of a novel p97/valosin-containing protein-interacting motif of gp78 in endoplasmic reticulum-associated degradation. *J Biol Chem* 281:35359–35368.
74. Fang S, et al. (2001) The tumor autocrine motility factor receptor, gp78, is a ubiquitin protein ligase implicated in degradation from the endoplasmic reticulum. *Proc Natl Acad Sci USA* 98:14422–14427.
75. Thrower JS, Hoffman L, Rechsteiner M, Pickart CM (2000) Recognition of the poly-ubiquitin proteolytic signal. *EMBO J* 19:94–102.
76. Dong KC, et al. (2011) Preparation of distinct ubiquitin chain reagents of high purity and yield. *Structure* 19:1053–1063.
77. Martínez-Fonts K, Matouschek A (2016) A rapid and versatile method for generating proteins with defined ubiquitin chains. *Biochemistry* 55:1898–1908.
78. Fenton WA, Kashi Y, Furtak K, Horwich AL (1994) Residues in chaperonin GroEL required for polypeptide binding and release. *Nature* 371:614–619.
79. Bandau S, Knebel A, Gage ZO, Wood NT, Alexandru G (2012) UBXL7 docks on neddylated cullin complexes using its UIM motif and causes HIF1 α accumulation. *BMC Biol* 10:36.
80. Magnaghi P, et al. (2013) Covalent and allosteric inhibitors of the ATPase VCP/p97 induce cancer cell death. *Nat Chem Biol* 9:548–556.
81. Anderson DJ, et al. (2015) Targeting the AAA ATPase p97 as an approach to treat cancer through disruption of protein homeostasis. *Cancer Cell* 28:653–665.
82. Dai RM, Li CC (2001) Valosin-containing protein is a multi-ubiquitin chain-targeting factor required in ubiquitin-proteasome degradation. *Nat Cell Biol* 3:740–744.
83. Rothballer A, Tzvetkov N, Zwickl P (2007) Mutations in p97/VCP induce unfolding activity. *FEBS Lett* 581:1197–1201.
84. Barthelme D, Sauer RT (2013) Bipartite determinants mediate an evolutionarily conserved interaction between Cdc48 and the 20S peptidase. *Proc Natl Acad Sci USA* 110:3327–3332.
85. Meyer H-J, Rape M (2014) Enhanced protein degradation by branched ubiquitin chains. *Cell* 157:910–921.
86. Xu P, et al. (2009) Quantitative proteomics reveals the function of unconventional ubiquitin chains in proteasomal degradation. *Cell* 137:133–145.
87. Zhang Z, et al. (2013) Ter94 ATPase complex targets k11-linked ubiquitinated ci to proteasomes for partial degradation. *Dev Cell* 25:636–644.
88. Zhang Z, et al. (2015) The transitional endoplasmic reticulum ATPase p97 regulates the alternative nuclear factor NF- κ B signaling via partial degradation of the NF- κ B subunit p100. *J Biol Chem* 290:19558–19568.
89. Liu C, Liu W, Ye Y, Li W (2017) Ufd2p synthesizes branched ubiquitin chains to promote the degradation of substrates modified with atypical chains. *Nat Commun* 8:14274.
90. Ewens CA, et al. (2014) The p97-FAF1 protein complex reveals a common mode of p97 adaptor binding. *J Biol Chem* 289:12077–12084.
91. Hänzelmann P, Schindelin H (2011) The structural and functional basis of the p97/valosin-containing protein (VCP)-interacting motif (VIM): Mutually exclusive binding of cofactors to the N-terminal domain of p97. *J Biol Chem* 286:38679–38690.
92. Schubert C, Buchberger A (2005) Membrane-bound Ubx2 recruits Cdc48 to ubiquitin ligases and their substrates to ensure efficient ER-associated protein degradation. *Nat Cell Biol* 7:999–1006.
93. Beuron F, et al. (2006) Conformational changes in the AAA ATPase p97-p47 adaptor complex. *EMBO J* 25:1967–1976.
94. Song C, Wang Q, Song C, Rogers TJ (2015) Valosin-containing protein (VCP/p97) is capable of unfolding polyubiquitinated proteins through its ATPase domains. *Biochem Biophys Res Commun* 463:453–457.
95. Thoms S (2002) Cdc48 can distinguish between native and non-native proteins in the absence of cofactors. *FEBS Lett* 520:107–110.
96. Chang Y-C, et al. (2011) Pathogenic VCP/TER94 alleles are dominant actives and contribute to neurodegeneration by altering cellular ATP level in a *Drosophila* IBMPPD model. *PLoS Genet* 7:e1001288.
97. Shorter J (2017) Designer protein disaggregases to counter neurodegenerative disease. *Curr Opin Genet Dev* 44:1–8.
98. Carvalho AF, et al. (2012) High-yield expression in *Escherichia coli* and purification of mouse ubiquitin-activating enzyme E1. *Mol Biotechnol* 51:254–261.
99. Xue L, et al. (2016) Valosin-containing protein (VCP)-adaptor interactions are exceptionally dynamic and subject to differential modulation by a VCP inhibitor. *Mol Cell Proteomics* 15:2970–2986.
100. Hänzelmann P, Buchberger A, Schindelin H (2011) Hierarchical binding of cofactors to the AAA ATPase p97. *Structure* 19:833–843.